Structure and electrical properties of PAni.CSA/PMMA nanofibers prepared by electrospinning method

TARIQ J. ALWAN*, FATIMA S. JALI
Physics Department, College of Education, Al-Mustansiriyah University, Baghdad, Iraq

The nanofibers are considered as one of the types of one-dimensional nanomaterials, which have numerous advantages when compared to conventional fibers. The PAni.CSA/PMMA nanofibers was produced successfully by using the electrospinning method, and to know the control conditions of the size, structure and morphology of PAni.CSA/PMMA nanofibers, they were studied under the effect of the zone length between the needle and target, and applied voltage parameters. The AFM and SEM were used to study the morphology and the average diameters of the nanofibers. The smallest value of nanofibers average diameters was when the applied voltage 20 KV, the flow rate was 5 ml/h and 10 cm the zone length between the needle and target. The structure and electrical properties of nanofibers were also studied.

(Received April 24, 2017; accepted February 12, 2018)

Keywords: Electrospinning, PAni.CSA/PMMA, Nanofibers, Polyaniline

1. Introduction

In the last few years, conductive polymers have received a great interest by researchers, because they have an electronic, magnetic, and optical properties analogous to metals while preserving the environmental stability, flexibility and processability of the conventional polymers [1]. The conducting polymers have a great advantage, like simple synthesis, with their chemical structure which formed to change their physical properties, that's appropriate for low cost electronic devices [2][3]. Electrostatic generation of nanofibers ''electro-spinning'' has been recognized since the 1930, when an electrostatic technique, a high electric field is created between a polymer fluid included in a syringe with a capillary tip and a metallic collection, the product fibers are collected on the collection [4]. Electrospinning has gained much interest in the last decade, not only due to its flexibility in spinning different types of polymeric fibers, but also in its consistency in producing fibers in the subnano range. The nanofibers with smaller pores and a higher surface area than ordinary fibers have a massive applications in filtration, protective clothing, filtration, tissue scaffolds and optical electronics [5]. Electrospinning is using this technique for nano-polymeric fiber connector by many researchers to improve the specifications conductive polymers manufactured in the nanoscale fibers and make it more suitable for practical applications [6]. Some electrospinning technique has used rotating cylinder collector at a high round speed, because the electrospun nanofibers could be in alignment with the oriented circumferentially, and this gives the nanofibers other advantages [7]. The solutions of conductive polymers have low viscosity, Wherefore, be blended with other polymers to form a polymer solution has enough viscosity for spinning [8]. This research describes the fabrication and characterization of nanofibers of Poly(methyl methacrylate) (PMMA) which blended with polyaniline (PAni.CSA) by using electrospinning technique.

2. Experimental

The Polyaniline emeraldine base was synthesized by the oxidation polymerization of aniline in acidic media [9][10]. 100 mg of PAni emeraldine base was mixed with 130 mg of camphorsulfonic acid CSA, and dissolved in 10 ml chloroform $CHC1_3$, this solution is put under stirring for 8 hours. The resulting dark green solution was filtered. Poly methyl methacrylate PMMA with molecular weight 350000 was added to assist to form the fiber with weight ratio concentration 2.89 %. This solution was used to prepare the nanofibers by using electrospinning setup.The main components of the electrospinning technique can be classified as (i) syringe and syringe pump (ii) high voltage power supply and (iii) rotating a cylinder aluminum collector. The polymer solution is loaded in the syringe its needle connected to the positive terminal of the high voltage power supply, the negative terminal connected to the collector. The effect of preparation conditions on the prepared nanofibers, are given in Table 1, with needle gauge 23G and rotating speed of cylinder 1000 rmp. The morphology, nanofibers diameters and alignment of the PAni.CSA/PMMA nanofibers are investigated by employing Atomic force microscopy AFM (Nanosurf NaioAFM) and Scanning electron microscope SEM (a Hitachi S-4160 SEM). Structure characterization of the prepared PAni.CSA/PMMA nanofibers are investigated by using Philips X-ray diffraction diffractometer that have the following lineaments: source Cu, the current was at 30 mA, the voltage was at 40 KV and the wavelength λ=1.5405 A. The characterization bonds for the functional

groupes are measured by Fourier Transform Infrared FT-IR spectra (FTIR-600FT-IR Spectrometer, SIDCO England), where all spectra were recorded between 4000-400 cm^{-1}.

Table 1. Electrospinning conditions of preparation PAni.CSA/PMMA nanofibers

PMMA Concentration wt%	Voltage KV (V)	Flow rate ml/min	Gap distance cm (D)
2.89	10	5	10
			15
			20
2.89	10	5	10
	15		
	20		

3. Result and discussion

- **Morphology of alignment nanofibers**

The nanofibers diameters, morphology, and alignment of the PAni.CSA/PMMA nanofibers were examined by using AFM and SEM, and it was found that the prepared nanofibers have diameters ranging between 1.5 μm to about 30 nm. Both images of AFM and SEM showed that the all samples have good uniaxially aligned nanofibers. Those images also showed that the prepared nanofibers dose not including defects such as beads; but they have a good uniform thickness and are relatively smooth along the nanofibers. Fig. 1 shows the effect of the distance between the collector and the tip of the syringe on the prepared PAni.CSA/PMMA nanofibers, when the other conditions are fixed. The average diameters of nanofibers are reduced with the increase of the distance between the collector and the tip of the syringe and it was 46.32 nm at 10 cm distance, decreasing to 35.85 nm at 20 cm distance, see Table 2. It has proven that the distance affected on the nanofibers diameters, if the distance is very short, the fiber will not have enough interval time to convert to solid before arriving to the collector, while if the distance will be longer, the bead fiber can be acquired, so the optimum distance is recommended [11]. When decreasing the distance, this means, cutting short flight times and the time evaporation of solvent, and raising the electric field strength, which its outcome will leads to the increase of bead formation. The increase in distance will allow more time for the fluid jet to stretch fully and for the solvent to evaporate completely, by increasing more in the distance, the collected nanofibres are dried and fully stretched, so the fiber diameter will be reduced [12]. Fig. 2 shows the AFM images of PAni.CSA/PMMA nanofibers with different applied voltage 10, 15 and 20 KV. From this figures, it was clearly observed that the PAni.CSA/PMMA nanofibers, displayed an uniaxially aligned nanofibers. Accordingly, the increasing of applied voltage leads to reduce the average diameters of nanofibers, and the 20 KV of applied voltage appears that have smallest average diameters “about 34.156 nm”, and the better alignment. In the electrospinning method, the crucial factor is the applied voltage, only the applied voltage which is higher than the threshold voltage, that charged jets is ejected from Taylor Cone, can be occurred [13]. Many groups indicated that the higher voltages lead to raise the electrostatic repulsive force on the charged jet, for favouring the decreasing of fiber diameter. The PAni.CSA/PMMA nanofibers are prepared at flow rate 5 ml/hr, distance 10 cm and applied voltage 20 KV, were analyzed by SEM.

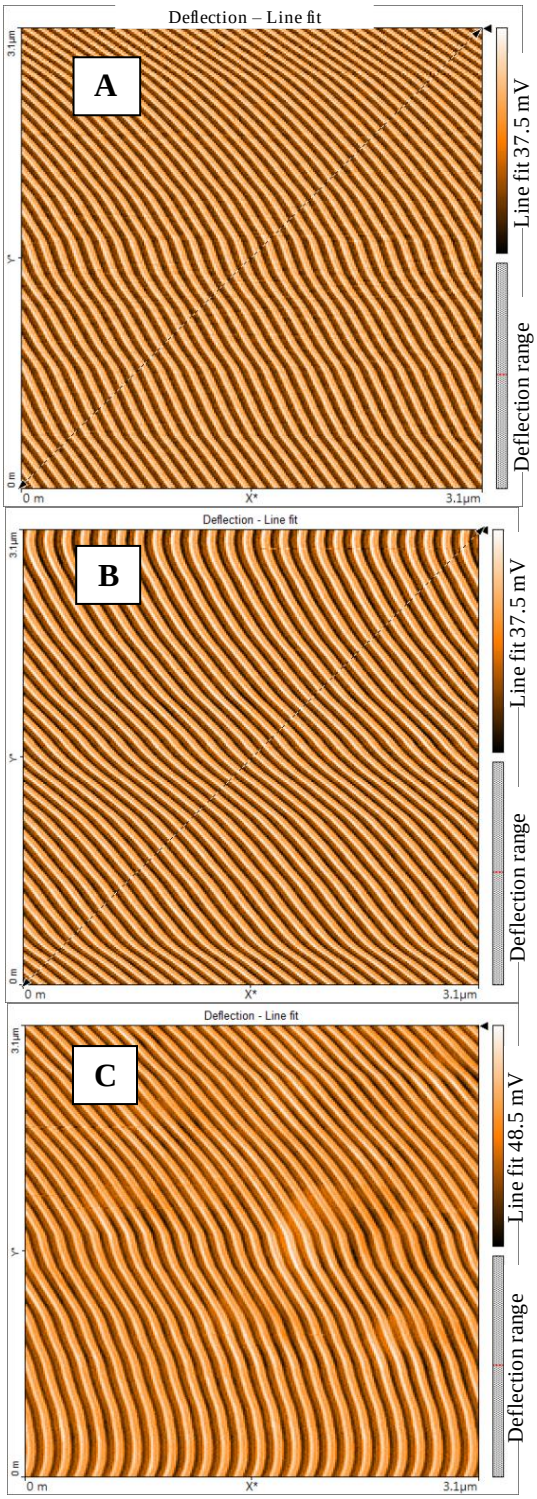

Fig. 1. AFM morphology for electrospun nanofibers of PAni.CSA/PMMA at a) 10 cm b) 15 cm c) 20 cm

Table 2. The structure parameters of PAni.CSA/PMMA nanofibers

Volt=10 KV R=5 m/h				
D cm	*Nanofibers diameters nm*	C.S A^o	*d-space* (A^o)	σ $S.cm^{-1}$
10	46.32	14.27	2.065	6.06E-6
15	38.37	42.42	2.815	6.86E-6
20	35.85	52.38	2.817	7.29E-6
D=10 R =5 ml/h				
(V) KV	*Nanofibers diameters nm*	C.S A^o	*d-space* A^o	σ $S.cm^{-1}$
10	46.32	14.27	2.065	6.070E-6
15	40.01	15.29	3.828	7.399E-6
20	34.16	52.27	2.817	8.312E-6

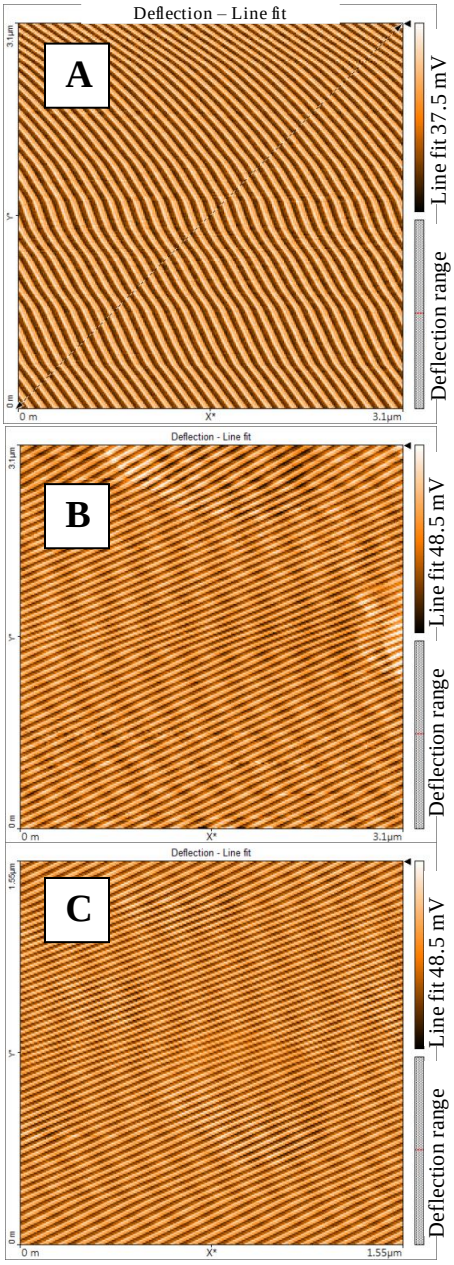

Fig. 2. AFM morphology for electrospun nanofibers of PAni.CSA/PMMA at a) 10 KV b) 15 KV c) 20 KV

The SEM images of nanfibers are shown in Fig. 3, the nanofibers were imaged with 30 KV voltages and X10-20 K. These images have great conformity with the AFM analysis results about the diameters of nanofibers and the other morphology notes. The prevailing morphology in all samples, as observed in the Figs. 1-2-3, but in some rare locations in the several samples observes some porous nanofibers with micro diameters as shown in Fig. 4. The production of these fibers may be outcoming due to gradual increasing of the applied voltage when it begins the electrospinning process, that is produced at the first moments of the star applied the voltages. The porous nanofibers can be generated by choosing particular solvents or solvent mixtures [14], polymer is blended under controlled environment mediums [15] and by changing the collector temperature [16]. A porous nanofiber improves performance for many applications, because of their high surface area. The nanostructure provides a high interfacial area, which is essential for achieving high-quality pores [17]. The formation of porous fibers by using electrospinning, means that the surface area of the fiber mesh can be more increased [14]. Megelski S. *et al.*, 2002 [18] studied the influence of electrospinning parameters like as flow rate, applied voltage, and distance on morphology of porous. They noticed the average pore size will grow by the increase of the flow rate, while the pore formation and size are not influenced by changing the distance as well as the voltage. Adnan Haider *et al.*, 2015 [19] and Viness Pillay *et al.*, 2013 [20] also observed the shape and pores size affected by changes the preparation parameters of electrospinning process.

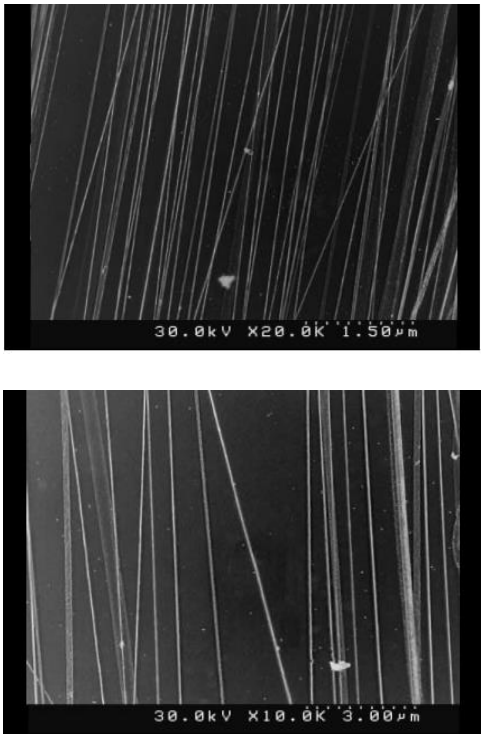

Fig. 3. SEM images of PAni.CSA/PMMA nanofibers at flow rate 5 ml/hr, distance 10 cm and applied voltage 20 KV

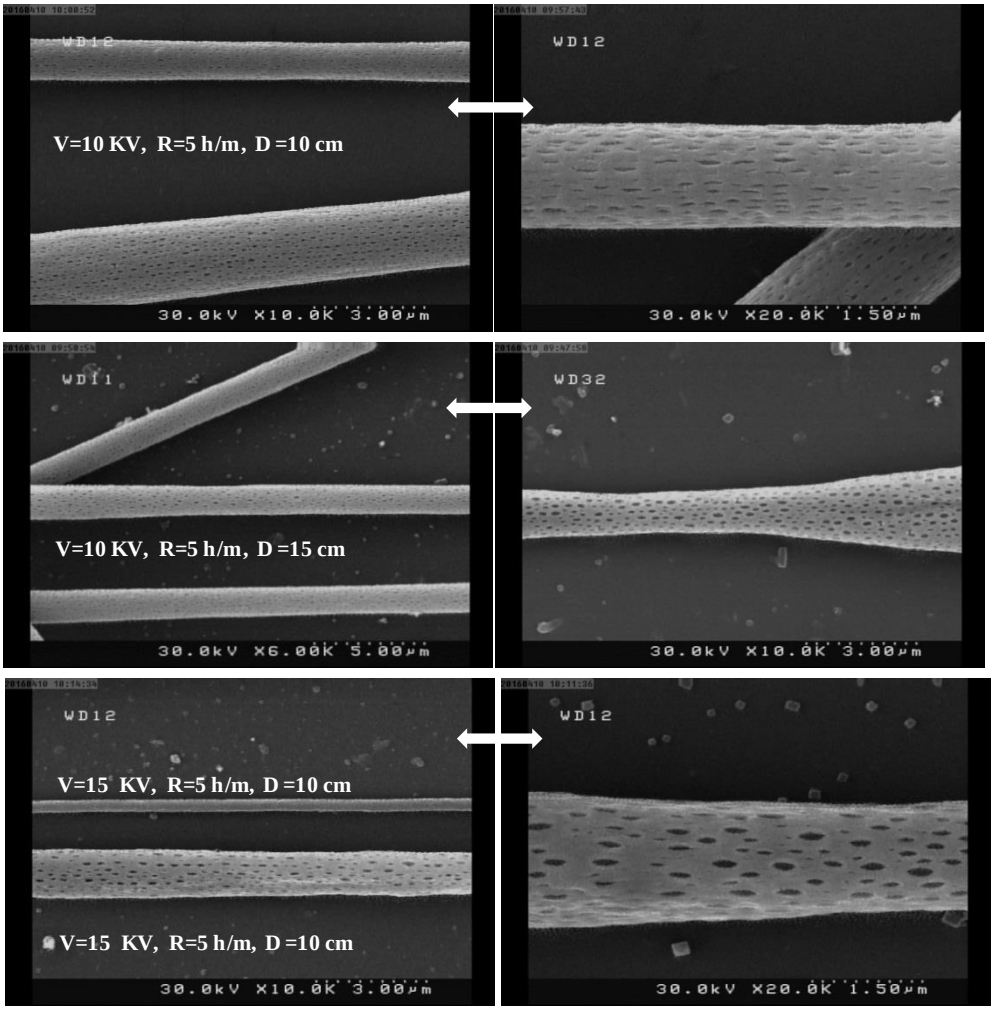

Fig. 4. The SEM images for PAni.CSA/PMMA nanofibers at different preparation conduction

- **X-Ray diffraction**

The XRD figures recorded for the PAni.CSA/PMMA nanofibers with the effect of distance between the collector and the tip of the syringe, 10, 15 and 20 cm are shown in Fig. 5. The X-ray patterns of PAni.CSA/PMMA nanofibers, shows a number of sharp peaks, this suggests a polycrystalline nature, the PAni.CSA/PMMA nanofibers are prepared at 10 and 15 cm have peak corresponding to PAni structure at $2\theta=44^{o}$, this agreed with Abdelaziz Rahy *et al*., 2008 [21] and Jorge Enrique *et al*., 2013 [22]. The sample that prepared at 15 cm has another peak corresponding to the (100) reflection of the PAni.CSA structure at $2\theta=33^{o}$ and this agreed with Sanjay L. Patil *et al*., 2012 [23]. When the distance increase to 20 cm, it is observed that the structure of nanofibers will transform from polycrystalline to single crystalline, where noticed only one peak characteristic of crystalline at $2\theta=44^{o}$ with a d spacing 2.817 A^{o}, and this agreed with Sanjay L. Patil *et al*., 2012 [23] Olubayode Ero-Phillips *et al*., 2012 [24], and Tariq J. Alwan *et al*., 2013 [7], where the increase of the distance in electrospinning method has improved the crystallinity structure of the polymer. Fig. 6 shows X-ray diffraction patterns of the PAni.CSA/PMMA nanofibers at different applied voltages 10, 15, 20 KV. The diffraction pattern of 5 and 10 KV PAni.CSA/PMMA nanofibers showed only one peak characteristic of crystalline at $2\theta=43.4^{o}$, this peak will disappear after the increase of the applied voltage to 20 KV as show in Fig. 6, but can be found growthing new strong peak at $2\theta=31.5^{o}$ assigned as (100) reflections, where the increasing of applied voltage changed the crystalline orientation and this confirms by shift of the position of the scattering peak from $2\theta=43.4^{o}$ to 31.5^{o} that corresponds (100) reflections, Moreover, the intensity of the peak has increased with increasing applied voltage. These may be due to the applied voltage to accelerate and stretch the polymer jet and overcome the surface tension of polymer solution [25], and this is meaning that increasing of voltages has improved the crystallinity of the PAni.CSA/PMMA nanofibers.

The average crystallite size (C.S) of PAni.CSA/PMMA nanofibers can be calculated from the X –ray spectrum by means of Full Width at Half Maximum (FWHM), by using Scherrer equation [26]:

$$C.S. = \frac{A\lambda}{\Delta\theta \cos\theta}$$

Where A Scherrer constant, commonly assume A =1, $\Delta\theta$ is the full – width at half maximum of the XRD peak appearing at the diffraction angle θ. The results of average crystallite size can be shown in Table (2), from this table can be noticed that the crystallite size increases with increasing distance, because the nanaofibers will have sufficient time to solidify before arriving to the collector, which be due to improve the crystalline structure during formation of the nanofibers [27]. When increasing the applied voltages, it has observed increasing the crystallite size, this leads to prove about the influence of applied voltage, favoring the narrowing of fiber diameter, and thus lead to improve the crystallization state and increasing of crystallite size.

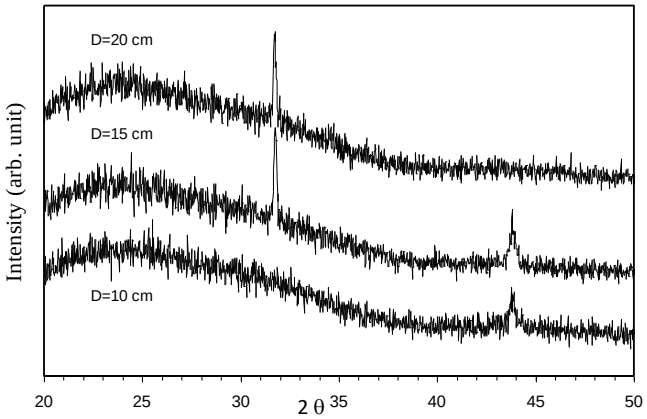

Fig. 5. The XRD spectra of PAni.CSA/PMMA nanofibers at different distances

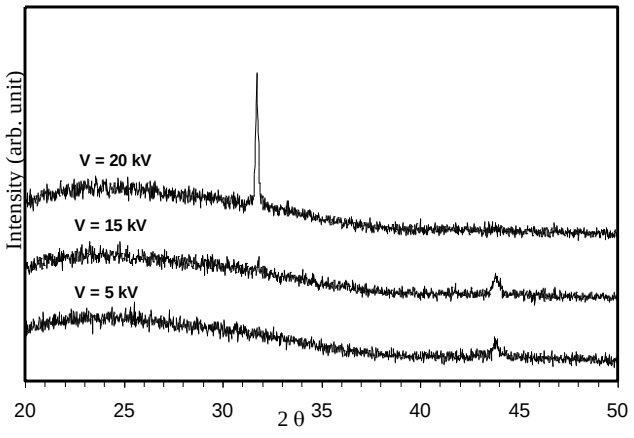

Fig. 6. The XRD spectra of nanofibers electrospun from PAni.CSA/PMMA at different apply voltage

- **FT-IR spectroscopy**

Infrared spectroscopy (IR spectroscopy) is a technique that is used to identify chemical compounds based on the way infrared radiation, and is absorbed by the compound [28]. The FTIR spectra of PMMA are shown in Fig. (7), that indicates to the details of functional groups present in the PMMA. In the pure PMMA spectrum a clear band appears at 1732 cm^{-1} this is possibly due to the C=O of PMMA which is appeared due to the presence of ester carbonyl group stretching vibration [29]. The C=O bond in plane and out of plane bending is assigned to band at 808 cm^{-1} and band at 756 cm^{-1} respectively [30], the peaks of 1151cm^{-1} is assigned O-CH_3 stretching [31], the asymmetric stretches and the symmetric stretches of the methyl CH_3 group in one structural repeat unit have appeared at 2848, 2951 and 2993 cm^{-1}, respectively [30]. Fig. (8) shows the FTIR spectra of PAni.CSA, and it is similar to those reported in earlier studies [32], which represent the appearance of ideal pattern of wave number for carbonyl group, they are observed at 1489 cm^{-1} C=C stretching of the quinoid ring, and the peak at 1438 cm^{-1} refer to C=C stretching of the benzenoid ring [33][34], the peaks appear at 3340 cm^{-1} and 3562 cm^{-1} refer to N-H stretching, while the observed peaks at 1142 cm^{-1}, 1192 cm^{-1}, 1224 cm^{-1}, 1279 cm^{-1} indicate to C-N stretching [35]. Two new peaks are shown at 1724 and 1070 cm^{-1} refer to C=O and SO^{+3} respectively [36]. The FTIR spectra of PAni.CSA/PMMA nanofibers shows in the Fig. (9) from this data it is clear that new peaks is corresponding to PMMA which are observed in the blended polyaniline. The appearance of new peaks with changes in present peaks directly indicates to the blend formation. For example the absorption band for a C=O shifted and will be more intense for a compound PAni.CSA/PMMA more than PAni.CSA. it is noticed appearance of a new peak at 1685cm^{-1} refer to (α,β-unsaturated) [37]. These alterations can be appointed to the construction of hydrogen bonding between these groups as a result of H donation in NH group. The H-bonding provide harmonization between polyaniline and carbonyl group in PMMA and develops the formation of an inter-penetrating network of polyaniline and the matrix chain [38].

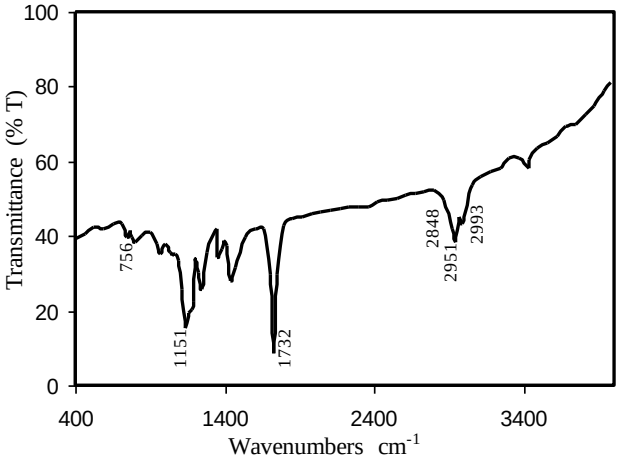

Fig. 7. The FT-IR spectra of PMMA

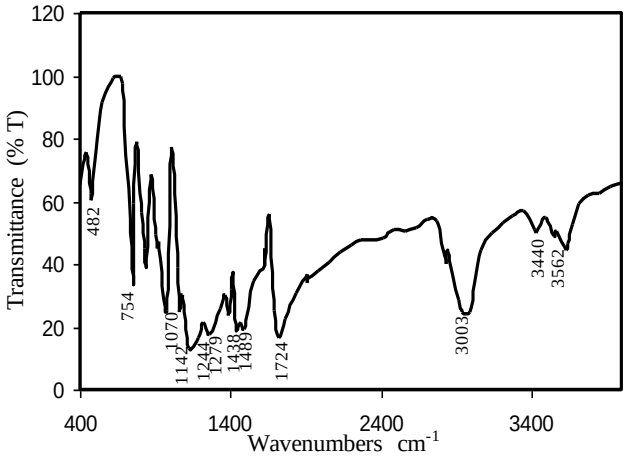

Fig. 8. The FT-IR spectra of PAni.CSA

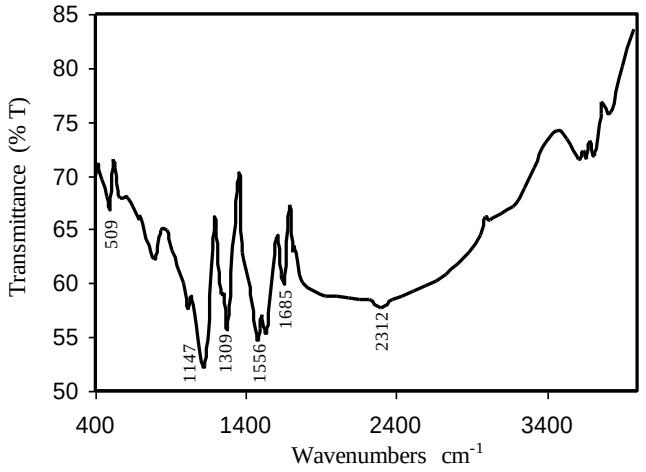

Fig. 9. The FT-IR spectra of PAni.CSA/PMMA

- **Electrical properties**

This section has studies the electrical properties for PAni.CSA/PMMA nanofibers. The effects of distance between the needle and collector, and applied voltage parameters on the electrical conductivity of nanofibers were investigated. The process of determining the mechanism of the electrical conductivity is still complicated due to the overlapping mechanisms of electrical conductivity between them as well as the transmission of charges carriers within the material and travels over the surface between the polymer and the electrodes [39]. The process of determining the mechanism of electrical conductivity in polymers depends on the study of (voltage - current) characteristics. It is difficult to measure the I-V characteristics of single nanofiber, because the isolating a single fiber actually is a difficult task, there is one way to bypass this difficulty, by taking a few number of nanofibers to be formed a layer, and then depositing two metallic electrodes (Al) for the measurement. The current-voltage characteristic of PAni.CSA/PMMA nanofibers at different distances between the needle and collector, and at different applied voltage are shown in Fig. 10 and 11. The I-V curve shows ohmic behavior at all applied voltage (V) for all samples. The electric conductivity is calculated by equation [40]:

$$\sigma = \frac{L}{R\,A}$$

Where R is the resistance of length L of the layer with cross-sectional area A, the unit of conductivity is thus S. cm^{-1}, and values of conductivity are tabulated at Table 2. From this table it has since noted the electrical conductivity increasing with increases the distances, from 6.06×10^{-6} S.cm^{-1} at a distance 10 cm to 7.29×10^{-6} S.cm^{-1} at a distance 20 cm, this increase due to reduce of nanofibers diameters and enhance the structures properties with increasing the distances, and this agreed with A. S. Sarac 2012 [41] S. Konagaya *et al*., 2014 [42] V. Jacobs *et al*., 2010 [43]. Also from Table 2 has observed the

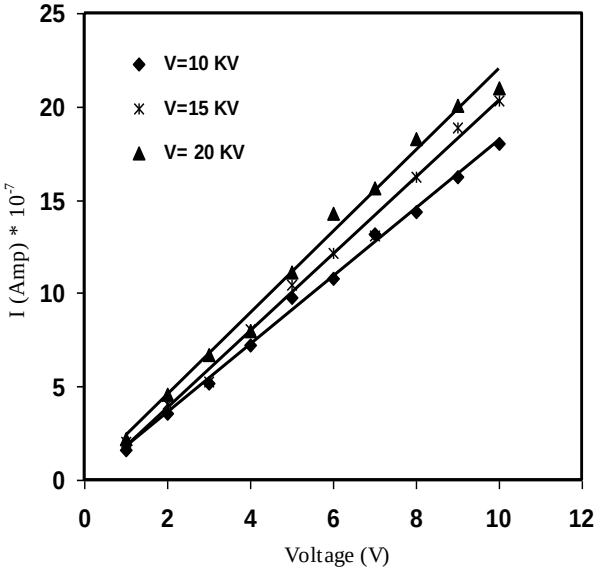

Fig. 10. The Current-voltage characteristic for PAni.CSA/PMMA nanofibers at different voltages

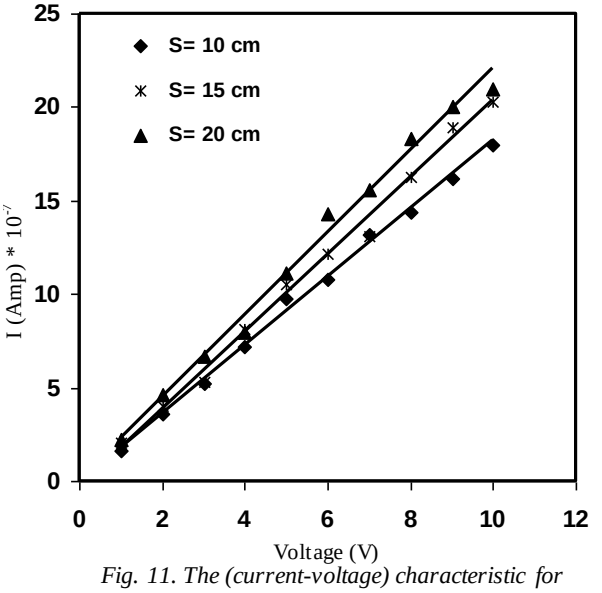

Fig. 11. The (current-voltage) characteristic for PAni.CSA/PMMA nanofibers at different distants

Increasing electrical conductivity when raiseing the applied voltages, from the 6.07×10^{-6} $S.cm^{-1}$ at voltage 10 KV to 8.312×10^{-6} $S.cm^{-1}$ at voltage 20 KV, this increasing in electrical conductivity due to the same raison that mention above, about the enhancement of the electrical conductivity with decreasing the nanofibers diameters. On the other hand, the enhancement of electrical conductivity of polymeric materials depends on their crystalline structure [44]. As reported by Xi and Tang 2005 that mention the increase in the length of the chains (when increasing the crystalline) could increase the conductivity of the polymer [45].

4. Conclusion

The PAni.CSA/PMMA nanofibers, were produced successfully by using the electrospinning techniques. The effects of distances and applied voltage on, the nonfibers diameters, morphology, crystallinity, and functional groupes of electrospun PAni.CSA/PMMA nanofibers which were investigated. Results show that smallest diameter "34.16 nm" obtained at the applied voltage 20 KV with flow rate of 5 ml/h and 10 cm the zone length between the needle and target. The XRD data of these nanofibers show the high intensity and peaks sharpness confirm that this technique improve the crystallinity state of polymer, in addition average crystallite size increases with reducing the nanofiber diameters. The FTIR spectra showed the appearance of new peaks with changes in PMMA and PAni.CSA peaks, this directly indicates the blend between PAni.CSA and PMMA. finally, the electrical measurements show an improving in electrical properties of the PAni.CSA/PMMA nanofibers prepared by this method, with decrease the average diameters of nanofibers.

References

[1] H. M. Huang, Z. Y. Li, C. Wang, Solid State Phenomena **121-123**, 579 (2007).

[2] K. M. Zaidan, H. F. Hussein, R. A. Talib, A. K. Hassan, Energy Procedia **6**, 85 (2011).

[3] R. J. Tseng, Jiaxing Huang, Jianyong Ouyang, Richard B. Kaner, Yang Yang, Nano Letters **5**(6), 1077 2005).

[4] I. D. Norris, Manal M. Shaker, Frank K. Ko, Alan G. MacDiarmid, Synthetic Metals **114**, 109 (2000).

[5] T. Subbiah, G. S. Bhat, R. W. Tock, S. Parameswaran, S. S. Ramkumar, Journal of Applied Polymer Science **96**, 557 (2005).

[6] P. W. Gibson, Calvin Lee, Frank Ko, Darrell Reneker, Journal of Engineered Fibers and Fabrics **2**(2), 32 (2007).

[7] Tariq J. Alwan, Kareema M. Ziadan, Kadhum J. Kadhum, International Review of Physics (I.RE.PHY.) **7**(2), 185 (2013).

[8] K. Desai, C. Sung, NSTI-Nanotech **3**, 429 (2004).

[9] M. Jayakannan, P. Anilkumar, A. Sanju, European Polymer Journal **42**, 2623 (2006).

[10] R. A. Talib, M. Sc. Thesis, University of Basrah, College of Science, Physics Department, Basra, Iraq, (2009).

[11] Z. Li, C. Wang, One-Dimensional Nanostructures, Springer Briefs in Materials, (2013). DOI: 10.1007/978-3-642-36427-3-2.

[12] M. Chowdhury, George Stylios, International Journal of Basic & Applied Sciences IJBAS-IJENS **10**(6), 116 (2010).

[13] D. Aussawasathien, Ph.D Thesis, University of Akron, U.S.A., May, (2006).

[14] Wee-Eong Teo, Seeram Ramakrishna, Nanotechnology **17**, 89 (2006).

[15] M. M. Demir, eXPRESS Polymer Letters **4**, 2 (2010).

[16] Y. Qiu, Jie Yu, Xiaosong Zhou, Cuili Tan, Jing Yin, Nanoscale Res Lett. **4**(2), 173 (2009).

[17] L. Qie, Wei-Min Chen, Zhao-Hui Wang, Qing-Guo Shao, Xiang Li, Li-Xia Yuan, Xian-Luo Hu, Wu-Xing Zhang, Yun-Hui Huang, Adv. Mater. **24**, 2047 (2012).

[18] S. Megelski, Jean S. Stephens, D. Bruce Chase, John F. Rabolt, Macromolecules **35**, 8456 (2002).

[19] A. Haider, Sajjad Haider, Inn-Kyu Kang, Arabian Journal of Chemistry, (2015), DOI:

[20] V. Pillay, Clare Dott, Yahya E. Choonara, Charu Tyagi, Lomas Tomar, Pradeep Kumar, Lisa C. du Toit, Valence M. K. Ndesendo, Hindawi Publishing Corporation, Journal of Nanomaterials **2013**, 22 (2013).

[21] A. Rahy, Mohamed Sakrout, Sanjeev Manohar, Sung June Cho, John Ferraris, D. J. Yang, Chem. Mater. **20**, 4808 (2008).

[22] J. Enrique Osorio-Fuente, Carlos Gómez-Yáñez, María de los Ángeles Hernández-Pérez, Mónica de la Luz Corea-Téllez, J. Mex. Chem. Soc. **57**(4), 306 (2013).

[23] S. L. Patil, Manik A. Chougule, Shailesh G. Pawar, Shashwati Sen, Vikas B. Patil, Soft Nanoscience Letters **2**, 46 (2012).

[24] O. Ero-Phillips, Mike Jenkins, Artemis Stamboulis, Polymers **4**, 1331 (2012).

[25] S. Sangthaiyarak, N. Tawichai, K. Pengpat, G. Rujijanagul, T. Tunkasiri, S. Eitssayeam, Advanced Materials Research **506**, 262 (2012).

[26] B. D. Cullity, S. R. Stock, Elements of X-Ray Diffraction, 3th edition, Prentice-Hall in the United States of America, (2001).

[27] Tariq J Alwan, Ziad Abdulahad Toma, Muhsin A Kudhier, Kareema M Ziadan, Madridge J. Nano. Tec. Sci. **1**(1), 1 (2016).

[28] P. R. Griffiths, James A. De Haseth, Fourier Transform Infraed Spectrometry, Second Edition, Published by John Wiley & Sons, (2007).

[29] B. S. Kannan, V. Selvaraj, S. Rajeswari, Trends Biomater. Artif. Organs. **18**(1), 41 (2004).

[30] M. Rosemal H. Mas Harisa, S. Kathiresanb, S. Mohanc, Der Pharma Chemica **2**(4), 316 (2010).

[31] E. M. Abdelrazek, A. M. Hezma, A. El-khodary, A. M. Elzayat, Egyptian Journal of Basic and Applied

Sciences **3**, 10 (2016).
[32] Tariq. J. Alwan, Ph. D Thesis, AL-Mustansiriyah University College of Science, Physics Department, Iraq, (2014).
[33] S. D. Nagesa, M. Revanasiddappa, C. Basavaraja, T. Suresh, S. C. Raghavendra, Indian Journal of Engineering& Materials Sciences **20**, 435 (2013).
[34] P. L. B. Araujo, Katia A. S. Aquino, Elmo S. Araujo, Int. J. Low Radiation **4**(2), 149 (2007).
[35] F. D. R. Amado, L. F. Rodrigues Jr., M. A. S. Rodriguesb, A. M. Bernardes, J. Z. Ferreira, C. A. Ferreira, Desalination **186**, 199 (2005).
[36] M. Khalid, Milton A. Tumelero, Iuri. S. Brandt, Vinicius C. Zoldan, Jose J. S. Acuña, Andre A. Pasa, Hindawi Publishing Corporation, Indian Journal of Materials Science **2013**, 1 (2013).
[37] R. M. Silverstein, G. C. Bassler, T. C. Morrill, Spectrometric Identification of Organic Compounds, 4th ed, New York, John Wiley and Sons, (1981).
[38] K. Tomara, Suman Mahendiaa, Shyam Kumara, Advances in Applied Science Research **2**(2), 327 (2011).
[39] M. Abu-Abdeen, G. M. Nasr, H. M. Osman, A. I. Aboud, Egyptian Journal of Solids **25**(2), 275 (2002).
[40] R. Bartnikas, American Society for Testing and Taterials, ASTM Publication **2**, (1987).
[41] S. Sarac, J. Nanomed Nanotechol **3**(9), 77 (2012).
[42] S. Konagaya, K. Shimizu, M. Terada, T. Yamada, K. Sanada, O. Numata, G. Sugino, AIP Conf. Proc. (1593), 270 (2014).
[43] V. Jacobs, Rajesh D. Anandjiwala, Malik Maaza, Journal of Applied Polymer Science **115**, 3130 (2010).
[44] M. Abdallh, E. Bakir, E. Yousif, Journal of Saudi Chemical Society **18**, 387 (2014).
[45] J. Xi, X. Tang, Electrochim. Acta **50**(27), 5293 (2005).

*Corresponding author: tariqjaffer2000@yahoo.com